

## **General Disclaimer**

### **One or more of the Following Statements may affect this Document**

- This document has been reproduced from the best copy furnished by the organizational source. It is being released in the interest of making available as much information as possible.
- This document may contain data, which exceeds the sheet parameters. It was furnished in this condition by the organizational source and is the best copy available.
- This document may contain tone-on-tone or color graphs, charts and/or pictures, which have been reproduced in black and white.
- This document is paginated as submitted by the original source.
- Portions of this document are not fully legible due to the historical nature of some of the material. However, it is the best reproduction available from the original submission.

NASA TM X-71230

# PREDICTION AND MEASUREMENT OF RADIATION DAMAGE TO CMOS DEVICES ON BOARD SPACECRAFT

(NASA-TM-X-71230) PREDICTION AND  
MEASUREMENT OF RADIATION DAMAGE TO CMOS  
DEVICES ON BOARD SPACECRAFT (NASA) 10 p  
HC A02/MF A01

N77-13333

CSCI 09C



R. A. CLIFF  
V. DANCHENKO  
E. G. STASSINOPOULOS  
M. SING  
G. J. BRUCKER  
R. S. OHANIAN



OCTOBER 1976



————— **GODDARD SPACE FLIGHT CENTER** —————  
**GREENBELT, MARYLAND**

PREDICTION AND MEASUREMENT OF RADIATION DAMAGE  
TO CMOS DEVICES ON BOARD SPACECRAFT

R. A. Cliff  
V. Danchenko  
E. G. Stassinopoulos  
M. Sing  
G. J. Brucker  
R. S. Ohanian

October 1976

GODDARD SPACE FLIGHT CENTER  
Greenbelt, Maryland

## CONTENTS

	<u>Page</u>
Abstract . . . . .	1
1. Introduction . . . . .	1
2. Experimental Approach and Method . . . . .	1
3. Description of Devices . . . . .	2
4. Explorer-55 Spacecraft, Its Orbit and, CREM Instrument . . . . .	3
5. Space Radiation Environment for Explorer-55 . . . . .	4
6. Dose and Shielding Calculations . . . . .	5
7. On-the-ground Simulation and Calibration . . . . .	5
8. Flight Data Results . . . . .	6
9. Analysis and Discussion . . . . .	7
10. Conclusions . . . . .	7
Acknowledgments . . . . .	7
References . . . . .	7

R. A. Cliff, V. Danchenko, E. G. Stassinopoulos, and M. Sing  
Goddard Space Flight Center  
Greenbelt, Maryland

G. J. Brucker and R. S. Ohanian  
RCA Astro Electronics Division  
Princeton, New Jersey

REPRODUCIBILITY OF THE  
ORIGINAL PAGE IS POOR

### Abstract

The CMOS Radiation Effects Measurement (CREM) experiment is presently being flown on the Explorer-55. The purpose of the experiment is to evaluate device performance in the actual space radiation environment and to correlate the respective measurements to on-the-ground laboratory irradiation results. The experiment contains an assembly of C-MOS and P-MOS devices shielded in front over  $2\pi$  steradian by flat slabs of aluminum of 40, 80, 150, and 300 mils (1.02, 2.04, 3.81, and 7.62 mm) thicknesses, and by a practically infinite shield in the back. This paper presents initial results obtained from the CREM experiment. Predictions of radiation damage to C-MOS devices are based on standard environment models and computational techniques. A comparison of the shifts in CMOS threshold potentials, that is, those measured in space to those obtained from the on-the-ground simulation experiment with Co-60, indicates that the measured space damage is smaller than predicted by about a factor of 2-3 for thin shields ( $t < 100$  mils), but agrees well with predictions for thicker shields. It is not clear at this time how the trapped particle environment models or the computational methods should be modified in order to achieve better agreement between experimental results and predicted damage curves. A subsequent paper will present some considerations along these lines as well as an evaluation of performance of C-MOS devices located in a typical electronic subsystem box within the spacecraft.

### 1. Introduction

There are many advantages of Complementary Metal-Oxide-Semiconductor (C-MOS) integrated circuits (ICs) over bipolar ICs in the design of large scale integrated logic and memory circuitry for spacecraft. Among these are extreme compactness and low power consumption. Such circuits are being orbited to an ever increasing extent. C-MOS ICs, however, are found to be more sensitive to space radiation than their bipolar counterparts. The mechanism responsible for the radiation damage in C-MOS devices is that of ionization and charge accumulation in the gate oxide and at the semiconductor-insulator interface. These effects begin to appear about two orders of magnitude lower than the effects of semiconductor surface damage in bipolars. In addition, since charge accumulation in the gate oxide is cumulative, the radiation damage in C-MOS ICs has become of great concern as space missions become longer and longer.

The successful application of unhardened C-MOS devices in spacecraft which traverse the Earth's radiation belts may hence require shielding. Shielding, however, is very heavy, and therefore it is most desirable to minimize any excessive weight penalty. It has consequently become important for spacecraft designers to be able to predict accurately the anticipated radiation damage to C-MOS devices and to estimate closely the shielding requirements. Such predictions presuppose that the following three elements are known: (1) the energies of the particles encountered by the spacecraft,

(2) the shielding effectiveness of given materials for particles of various energies, and (3) the response of C-MOS devices to the radiation which is found inside the shield.

In regards to element (1) and considering the best radiation environment models available today, the electron intensities are only known to within a factor of 3 and the proton intensities to within a factor of 2. As to elements (2) and (3), the radiation damage in C-MOS as a function of dose in rads can of course be measured in the laboratory by using such radiation sources as Co-60 or monoenergetic electron accelerators. But this procedure only approximates the effects of charged particle fluxes with distinct spectral distributions. However, the error introduced into the results by this approximation is smaller than the uncertainty in the environment models. Besides, a reproduction of the actual space radiation spectra in the laboratory, even if the environment were known to a much better accuracy, would be excessively complicated and expensive. In addition, there is a long-term annealing process (self healing) of radiation damage active in C-MOS devices which may be different in the space environment than on the ground.

To provide some of the data needed for more reliable predictions, the C-MOS Radiation Effects Measurements (CREM) experiment is presently being flown on the Explorer-55 (formerly designated AE-E) while simultaneously the necessary complementary measurements are being carried out on the ground. In this paper we present some significant and interesting preliminary results. As more data become available, a more detailed analysis and thorough evaluation will be performed and their findings presented in a subsequent report.

### 2. Experimental Approach and Method

The main objective of the CREM experiment is to measure the effect of space radiation on CMOS ICs and to verify the accuracy with which one can predict damage to semiconductor devices on board spacecraft by comparing the results with current environment model predictions and with the corresponding on the ground calibrations.

The specific devices used are n- and p-channel MOS transistors. The device-parameter of primary interest is the threshold potential shift,  $\Delta V_{GT}$ . Figure 1 outlines in a block diagram the major elements of the CREM experiment. The left hand branch depicts the process used to predict the expected shift in the device parameter  $\Delta V_{GT}$ , employed in the past with varying degrees of sophistication. For the CREM experiment, this process was implemented with special care in order to produce predictions as accurate as the state of the art would allow. The approach followed and the uncertainties involved are discussed in another section.

Since most predictions to date have been on an open-loop basis, with no subsequent verification of what actually

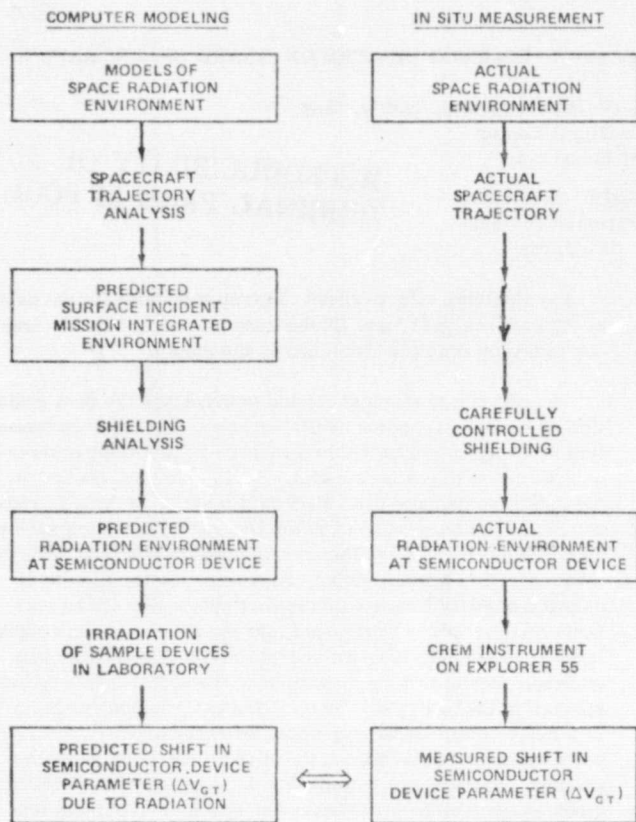


Figure 1. The CREM Experiment

happened in space, this experiment rectifies that situation by performing in orbit a carefully controlled measurement of the actual shift in threshold potential, as indicated by the right hand branch in Figure 1. Finally, the predicted shift is then compared to the actual shift, thereby either validating the accuracy of the predictions or providing information for their improvement. Since the objective of the experiment is based on measurement and comparison, the devices used must be chosen very carefully so that they will have the same response in radiation environments of the same ionization-producing dose. It would have been ideal to be able to first calibrate the devices and then use the same on board the spacecraft, but, as was shown<sup>1</sup> by one of the authors, the radiation response of MOS devices changes with repeated radiation and annealing cycles. The next best approach is to use devices which are manufactured in the same gate oxide growth process run. This is what was done. In addition, the device radiation response must cover a large radiation dose range in case of under or over prediction of the space radiation environment.

It is known that most of the MOS devices exhibit a long term annealing (some even show reverse annealing) of radiation damage as a function of temperature. Therefore, for the space flight results of the CREM to be meaningful, there must be a number of associative on-the-ground measurements and calibrations, such as on-the-ground simulation experiments whereby the long term annealing will be measured and accounted for.

The CREM experiment, therefore, consists of five major parts: (1) the flight apparatus that directly measures the effects of the space radiation on C-MOS devices under various

shieldings (4 defined and 1 estimated), (2) the laboratory simulation experiment with a Co-60 source, (3) prediction of the space radiation using the actual orbital parameters, (4) calculation of dose vs. depth curves, and (5) comparison of predicted damage to actual damage in the orbiting devices.

### 3. Description of Devices

Two MOS technologies were chosen for this experiment: The RCA COS/MOS unhardened or "soft" technology and the AMI p-MOS, high threshold variety. The reasons for choosing these two technologies are: (1) RCA's n-channels of the "soft" variety, when biased with 10 volts, already exhibit a measurable shift in the threshold potential (the gate bias measured at  $10\mu\text{A}$  drain current) after an exposure of about  $1 \times 10^3$  rad-silicon; this permits the measurement of radiation damage at lower ionization doses. At the same time, the p-channels of the RCA CD-4007 devices on the same chip of silicon are much less radiation-sensitive, when both biased and unbiased, and will cover the high portion of the dose range; (2) several sub-systems of the Explorer-55 spacecraft contain some RCA "soft" COS/MOS devices and it would be advantageous for the AE project to be able to monitor and predict possible radiation damage to the spacecraft circuitry during this mission, (3) the radiation-sensitivity of the p-channel AMI high-threshold devices (not ion-implanted) lies between that of the RCA biased or unbiased n- and p-channels. Aside from this, GSFC uses a considerable quantity of these devices in its missions and it will, therefore, be of great value to have direct measurements on them in the space environment.

#### a. RCA COS/MOS, Type CD 4007 AK/IR

The RCA COS/MOS integrated circuits (Type CD 4007) were manufactured by RCA in February 1974 and packaged in welded-seal ceramic flat packs with 5 mil (0.08 mm) Kovar lids [9 mil (0.2 mm) equivalent aluminum]. Each device contains 3 p-channel and 3 n-channel transistors which are individually accessible. The lot (No. 405) was guaranteed by the company to have originated from the same wafer, or from several wafers, but having been physically located next to each other in the same gate oxide growth run. This is important because for the experiment to be meaningful, the radiation-induced gate charge trapping capability of the gate oxides must be the same.

#### b. AMI p-channel, Type 585A

A wafer containing AMI p-channel, 10 channel switches, was manufactured by AMI in 1971 and diced and packaged at GSFC in flat packs with 10 mil (0.3 mm) Kovar lids [28 mil (0.7 mm) equivalent Al]. All the devices came from the same wafer. In this configuration, each device contains 10 individually accessible p-channel transistors (although only 6 of them were actively used). The threshold potentials were around -4 volts and the variation in the threshold potential from transistor to transistor in the same device was within 0.2 volts. In this particular technology the radiation response in the unbiased devices is greater than in the biased devices.

The uniformity of the charge trapping capability has been determined by irradiating 6 devices of each type with Co-60 gamma rays and with 1 MeV electrons. The variation in the shift of the threshold potentials ( $\Delta V_{GT}$ ) was found to be less than 5% from device to device in both technologies.

#### 4. Explorer-55 Spacecraft, Its Orbit and CREM Instrument

The Explorer-55 spacecraft was launched on November 19, 1975, and achieved an initially highly elliptical orbit with an apogee of 1,864 statute miles (3,000 kilometers) and a perigee of 98 miles (157 kilometers). The orbit is inclined 19.7° to the equator.

Because of its main objective of thermosphere exploration, the spacecraft's apogee was allowed to decrease by about 2 to 5 km per day until it was stabilized on May 15, 1976 with an apogee of 1,600 km and perigee of 151 km. On August 1, 1976, the orbit was again permitted to decay and should become circular in late October 1976.

The on-board CREM experiment consists of: (a) the device assembly, mounted flush with the solar array in the surface of the spacecraft and containing four device groups; (b) an additional fifth device group located within a typical electronics box inside the spacecraft; and (c) an on-board data acquisition system, also located inside the spacecraft.

Each device group contains 26 instrumented transistors: 6 AMI p-channels (one AMI 585A device), 10 RCA p-channels and 10 RCA n-channels (4 RCA CD 4007 devices). A total of  $5 \times 26 = 130$  instrumented transistors are in the CREM experiment on the spacecraft. The locations of the devices in the CREM device box are shown in Figure 2.

#### Shielding of Devices

The devices in the box are mounted on a printed circuit board with copper heat sink slabs bonded to the back of the board. This printed circuit board is assembled into the device box as follows: The board forms the front of a rectangular prism, the other 5 sides of which are made of 250 mil (6.4 mm) aluminum bonded to 250 mil (6.4 mm) thick tungsten. This gives a  $2\pi$  steradian back shield of equivalent thickness greater than 1.8 inch (4.6 cm) of aluminum. A front cover is mounted over the printed circuit board. This cover provides aluminum shields of thicknesses 40 mil (1.0 mm), 80 mil (2.0 mm), 150 mil (3.8 mm), and 300 mil (7.6 mm) designed in such a way that behind each shield thickness there is one group of four RCA CD 4007 devices and 1 AMI p-channel device. When calculating shield thicknesses, however, the device

packaging lids of 9 mil (0.2 mm) equivalent aluminum was added to each nominal slab thickness in the CREM box for the RCA devices; the AMI device package requires a value of 28 mil (0.7 mm) of Al. The entire device box was then mounted with the printed circuit board in the plane of the surface of the spacecraft. The device box in combination with the body of the spacecraft forms a  $2\pi$  steradian back shield, which in regards to electrons and low energy protons is for practical purposes infinitely thick compared to the front shields. However, high energy primary protons ( $E \geq 150$  MeV) will penetrate the back shield and contribute directly or indirectly (tertiary particles through secondary neutrons) to the damage of the devices. The front of the box has an unobstructed  $2\pi$  steradian view of the space environment.

#### Device Biasing

The electronics box on the spacecraft is designed to continuously apply a selected gate-to-substrate bias to each device except during the brief interval (1/2 second) during which that particular device is being measured. Of the 6 AMI transistors in each device group, 3 are at  $V_G = 0$  V and 3 are at  $V_G = -10$  V, constantly. Of the 10 RCA p-channel transistors in each device group, 2 are at  $V_G = 0$  V, 2 are at  $V_G = -10$  V, constantly, 4 are at  $V_G$  which is zero volts for half the orbit and  $-10$  V the other half of the orbit, and 2 are connected in a selfbiasing arrangement. (The duty cycled and self-biasing transistors will not be further discussed in this paper.) The 10 RCA n-channel transistors in each device group are biased like the 10 p-channel transistors except that  $V_G = +10$  V replaces  $V_G = -10$  V. Figure 3 shows the bias circuit for n-channel transistors.

#### Device Measurement

When the command to measure the devices is executed (from the ground or from an on-board programmer), the CREM electronics box automatically sequences through a complete measurement cycle of the 130 transistors. In each transistor, the 8 gate-to-substrate biases ( $V_G$ 's) required to produce 8 predetermined values of drain current ( $I_D$ ) are measured. They range from  $1 \mu\text{A}$  (nearly cut off) to  $3\text{mA}$  (actively switching) with intermediate current values of  $3 \mu\text{A}$ ,  $10 \mu\text{A}$ ,  $30 \mu\text{A}$ ,  $100 \mu\text{A}$ , and  $1\text{mA}$ . In this way I-V plots can be obtained for the individual n- and p-channel transistors. The

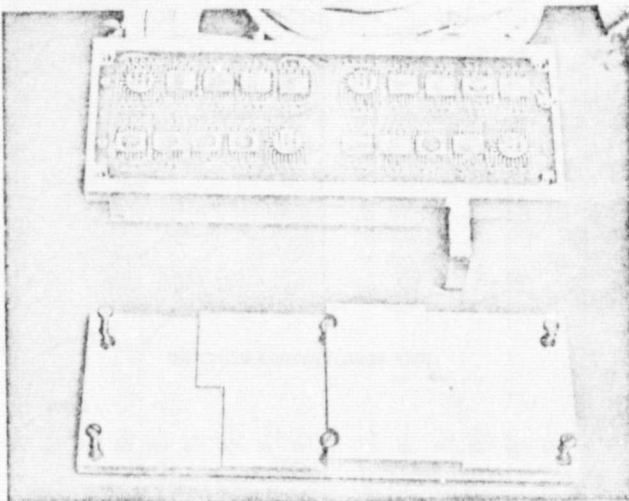


Figure 2. CREM Device Box and Its Cover

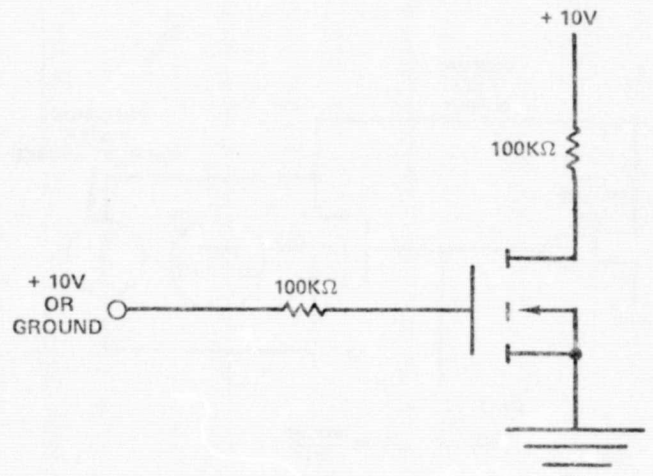


Figure 3. Biasing of n-channel Device During Irradiation

measurements are made by forcing the selected test current through the transistor and using an operational amplifier feedback circuit to adjust  $V_G$  to the value which maintains  $V_D = 10$  V. Figure 4 shows the circuits for n-channel transistors. In this discussion, only the essential elements of the measurement process have been covered; other elements (e.g., stability) which increase the complexity of the actual circuit, will not be considered here. The details of the measurement technique will be covered in a separate paper (to be published).

#### Measurement Accuracy

Considerable attention has been given to controlling and minimizing possible errors inherent in the measurements. Each device package is thermally bonded to a heat sink, thus keeping all the devices within  $1.4^\circ\text{C}$  of each other. Four thermistors are used to measure and telemeter the temperature of various parts of the heat sink in order to verify its proper function. Electrical switching, associated with the biasing and measurement function, is accomplished by using reed relays which, for practical purposes, act as ideal switches: zero resistance when closed and zero leakage when open. The measured gate voltage is sent directly to the telemetry system. The combined single-sample random errors and the quantization errors associated with the telemetry system are less than  $\pm 30$  mV. Several sources can contribute to errors in the values of the test currents, as for example, leakages in the back-biased parasitic diodes which exist on the sample IC chips. These would subtract from actual sample device current. However, both the thermally and radiation induced leakage are orders of magnitude smaller than the smallest test current used. The operational amplifier input current subtracts from the test current; however, the CREM instrument is calibrated prior to use and only the changes in this current introduce errors. Likewise, changes in operational amplifier offset voltage, and changes in precision current source reference voltage will introduce errors. An in-flight calibration scheme is employed to measure changes in each of these variables. The actual value of each test current is within  $\pm 16\%$  of the nominal value (the  $10\mu\text{A}$  test current is within  $\pm 1\%$  of its nominal value), but the actual value of each current is known and constant within  $\pm 1\%$ .

#### 5. Space Radiation Environment for Explorer-55

Starting from the launch date (November 19, 1975) and extending to mission day 159 (April 26, 1976), a continuous trajectory ephemeris was generated by the Telemetry

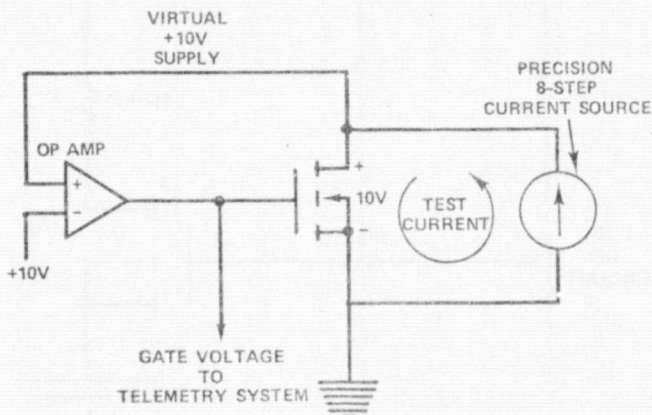


Figure 4. Measurement of n-channel Device

Computation Branch at Goddard, in which the actual satellite positions were defined in polar space at two-minute intervals. This continuous flight path description was divided into 159 trajectory segments of 24 hour duration that were subsequently converted into magnetic B-L space with McIlwain's INVAR program of 1965<sup>2</sup> and the field routine ALLMAG<sup>3</sup> utilizing the IGRF (1965) geomagnetic field model<sup>4</sup>. The field coefficients were extrapolated to the true mission epoch 1975.11 with linear time terms representing secular variation effects. Orbital flux integrations were then performed for each of these segments with the UNIFLUX system<sup>5</sup> using standard models of the environment: the appropriate for the launch epoch solar-min. versions of the AE5<sup>17</sup> and AE4<sup>6</sup> for the inner and outer zone electrons, and the AP6<sup>7</sup> and AP7<sup>8</sup> for the medium and high energy protons. All are static models which do not consider temporal variations. It should be noted that the AE5 does not contain any "Starfish" residuals because the artificial component contained in the experimental data used in the construction of the model, was exponentially decayed during the modelling process down to about background levels with lifetimes and cutoff times available as functions of energy and magnetic shell parameters  $L^9$ .

The daily electron and proton integration results are shown in Figures 5 and 6, respectively, for several energy levels. The data represent averaged, surface incident, omnidirectional, integral intensities. The periodic pattern in the contours is believed to be produced by the precession of the decaying eccentric orbit through the asymmetric (anomalous) geomagnetic geometry configuration. The trapped particle fluxes, predicted by the standard environment models for the Explorer-55 trajectory, do not seem to decline significantly for the first 150 days of the mission, although apogee altitude dropped from about 3000 km to about 1835 km. This is true for both species of particles, for all but the lowest energies plotted. After day 150, a more rapid decrease in the total daily intensities is indicated.

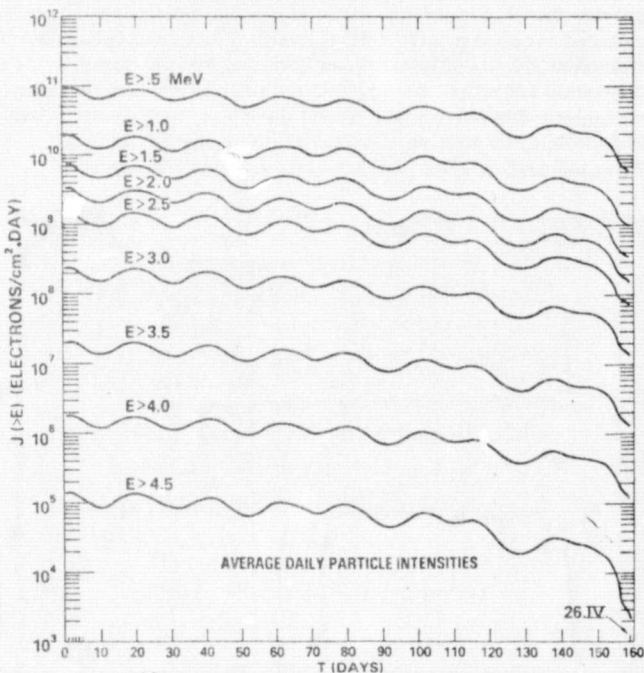


Figure 5. Time History of Mission Integrated, Omnidirectional, Integral, Trapped Electron Fluxes

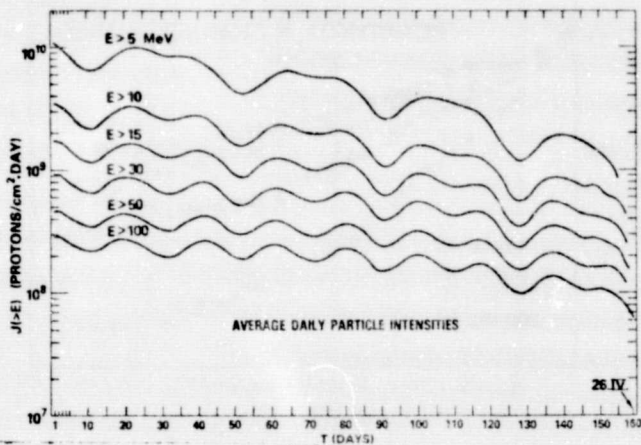


Figure 6. Time History of Mission Integrated, Omni-directional, Integral, Trapped Proton Fluxes

Solar flare protons are of no concern to this analysis because the mission is flying during the inactive period of the solar cycle.

#### 6. Dose and Shielding Calculations

In a previous paper<sup>10</sup>, the techniques for computing dose-depth curves for any assumed radiation environment were described. These techniques are applied to the radiation environments after 139 days in orbit, by using three different approximation methods: (1) one dimensional slab geometry, (2) three dimensional spherical geometry<sup>11</sup>, and (3) Monte Carlo technique<sup>12, 13, 14</sup>.

Figure 7 shows the total dose-depth curve after 139 days in orbit with all the contributing components, including bremsstrahlung, for the one dimensional slab geometry. Clearly, both electron and proton contributions towards the total dose for 40 mils (1.0 mm) and 80 mils (2.0 mm) shields are equally significant, whereas only protons contribute to the total dose for the 150 mils (3.8 mm) and 300 mils (7.6 mm) shields.

The relative importance of the individual components should not vary appreciably with computation method.

#### 7. On-the-ground Simulation and Calibration

In order to calibrate the space radiation environment against the Co-60 source, or vice versa, and in order to ascertain the extent of long-term annealing, the on-the-ground CREM experiment was started as soon as enough data had been received from space to establish the trend in the radiation damage there. The sample devices for this experiment were chosen, as previously described, to be as identical as possible to the ones on the CREM unit on board the spacecraft and the data were recorded in an identical way with the breadboard of the CREM instrument.

The on-the-ground simulation experiment involved the irradiation of one group of samples (i.e., a group of devices similar to the ones under each shield thickness on board the Explorer-55) every week with a weekly dose of Co-60 radiation in such a way as to effect the same radiation damage on the laboratory devices as the actual damage initially observed in space. Between weekly irradiations, the test devices were permitted to anneal at room temperature and under the same

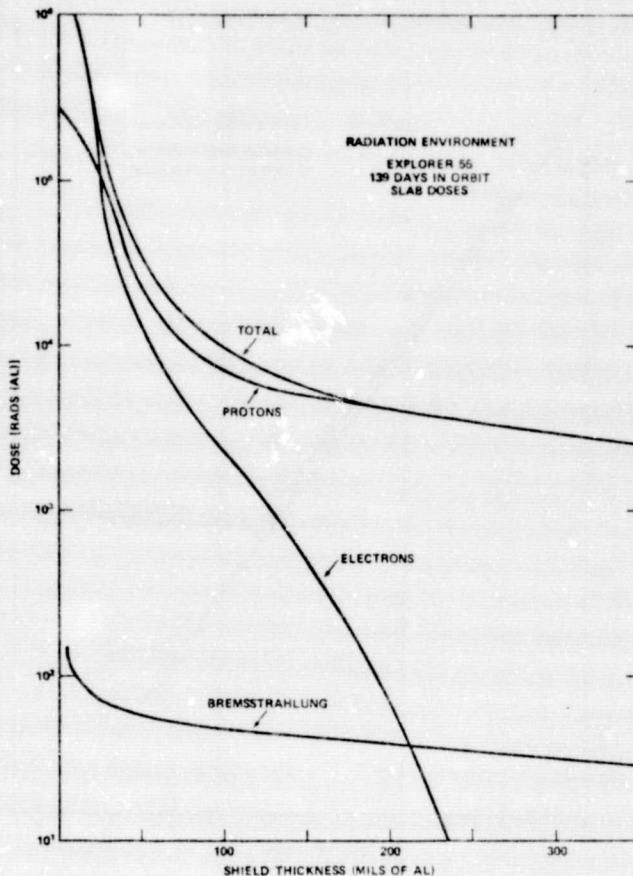


Figure 7. Contribution of Electrons, Protons, and Bremsstrahlung to the Total Dose-depth Curve

biasing configuration as in space. Data readings were taken regularly just before each next irradiation.

Since the range of temperature variation experienced by the CREM assembly in space is rather narrow (15°-30°C) and lies in the vicinity of room temperature, it is safe to assume, on the basis of earlier work<sup>15</sup>, that the degree of long term annealing, if any, will be similar in the present experiment, and that it can therefore be eliminated as an unknown quantity.

Some results of the calibration and simulation are shown in Figure 8 for biased RCA n-channels, where the circles relate to data obtained each week from the regularly irradiated devices (simulation). For comparison purposes, average results from a fast-rate radiation response on six n-channels of three independent samples, all irradiated so as to receive the entire corresponding dose within one day, are also given by the crosses. In this figure, gate biases for 10 μA currents are plotted against the total accumulated dose in rad-silicon. Space simulation samples were irradiated with a Co-60 dose rate of 0.15 rads/sec. Since there is a slight variation in the initial threshold potentials from device to device, the data were normalized to the same initial threshold potential. As can be seen from the graph, the radiation response for a biased n-channel is linear for both the fast and the simulation rate modes. In the simulation rate curve the lower circles are the threshold potentials immediately after the weekly irradiations and the upper ones are after weekly annealings, so that the true simulation rate response is represented by the

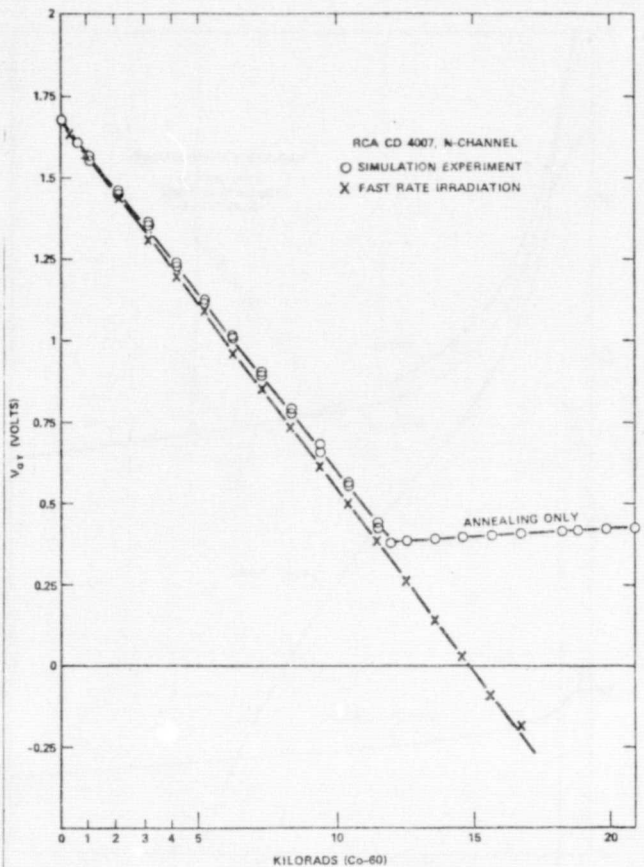


Figure 8. Radiation Response of RCA n-channel Transistor, Biased +10V

line drawn through the upper data circles. The samples of the on-the-ground experiments were subjected to the same radiation dose every week, because in this mission the orbit was continually changing and precise orbit parameters were not known a priori.

When it was observed that the total accumulated laboratory dose of  $1.2 \times 10^4$  rad-silicon exceeded the one experienced in space, the irradiations were stopped (see Figure 8) and only annealing is measured thereafter. As can be seen, the pure annealing also shows a linear behavior and constitutes about 0.9 mV per day for RCA biased n-channels. This very slow recovery characteristic of these RCA oxides has also been demonstrated elsewhere.<sup>16</sup>

### 8. Flight Data Results

The data of the flight experiment, as received from the spacecraft, consist of actual gate potential measurements for the 8 specified drain currents of the individual MOS transistors. The data shown in Figure 9 depict the shifts of the  $10 \mu\text{A}$  drain current gate potentials as a function of number of days in orbit. In comparison to the on-the-ground experiments where the radiation response for the biased n-channel is linear, the response in space is not linear. This is because the orbit of the Explorer-55 spacecraft was continually evolving into a less eccentric one with a corresponding decrease in energetic particle intensity encountered.

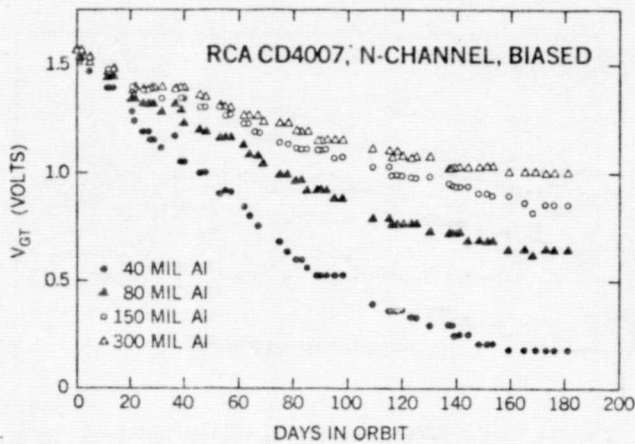


Figure 9. CREM Flight Data of RCA n-channel Transistors Under Various Shields

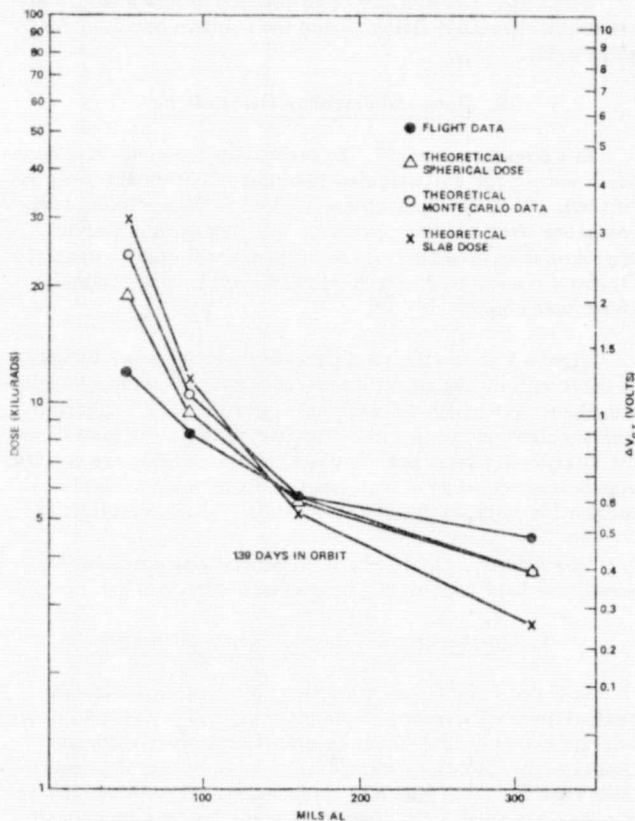


Figure 10. Comparison of Flight and Theoretical Data

The flight data for the 139 day mission were taken from Figure 9 and plotted in Figure 10 as a function of shield thickness in terms of both the shift in the threshold potential ( $\Delta V_{GT}$ ) on the right hand scale and the dose in rads-Si on the left hand scale. The values in rads-Si were obtained from the data in Figure 8 of the on-the-ground simulation experiment of the biased n-channel transistors, allowing for the appropriate

corrections for the small annealing observed in the laboratory. It should be recalled that these data were obtained from the degradation of n-channels biased with 10 volts and that the devices were exposed to worst case gate biasing conditions. Consequently, these larger threshold voltage shifts give a more sensitive measurement of ionization radiation. The unbiased n-channel and p-channel results are not yet usable since the threshold voltage shifts to date are too small.

## 9. Analysis and Discussion

It is estimated that the CREM flight data, such as shown in Figure 9, are correct to within 10%. This uncertainty is due mainly to the temperature variations of the devices during the data read-out and to a lesser extent due to errors in the CREM data acquisition system and the spacecraft's telemetry systems. The former is yet to be analyzed.

In the case of the on-the-ground simulation and calibration data, although the accuracy of the CREM breadboard is within 1%, Co-60 calibration is within 5%, and the variation from sample to sample was found to be also within 5%. The total error, therefore, is approximately within 10%.

To compare the results of the flight experiment with the predictions from the three computational methods, the values obtained from the latter were plotted directly as a function of dose in rads-Si and converted to the predicted shift in the threshold potential by using the on-the-ground simulation data of Figure 8.

Comparison of the theoretical infinite-back-shielded slab shifts with the spherical shifts of Figure 10 shows that the slab approximation overestimates the shifts at thin shields, that there is sufficient agreement at the intermediate shields, and that it underestimates the shifts at the thicker shields.

These preliminary results suggest that in the case of the n-channel biased devices, both the theoretical spherical and Monte Carlo methods have good agreement with the experimental flight results for the thick shields (Figure 10),  $t > 150$  mils, and poorer for the thin shields,  $t < 80$  mils. However, the maximum difference occurring at the thinnest shield of  $t \approx 50$  mils is not greater than a factor of three. Clearly, the uncertainty in the environment models of a factor of two for protons and three for electrons could account for the disagreement. The experimental results, flight and ground data, of the shift in the threshold potentials of RCA biased n-channel devices for the 139 day radiation exposure suggest either that the electron environment is overestimated by the models (the laboratory results of the shift in the threshold potentials are not produced by the space environment) or that the applied computational techniques are inaccurate, or both. The shift in the threshold potentials under the thick shields are due only to the high energy protons, as shown in Figure 7, and the techniques are more accurate for these particles than for the electrons. However, this experiment cannot eliminate either explanation.

## 10. Conclusions

The flight of the CREM experiment on board the Explorer-55 has been highly successful. All systems of the CREM instrument have been working well. From the preliminary results obtained so far the following may be concluded:

1. The experiment has clearly demonstrated that C-MOS damage measurements made with simple radioactive

sources in the laboratory, such as Co-60, may validly be used to predict changes in device properties affected by space environments consisting of charged particle fluxes (electrons and protons) distributed over wide energy ranges.

2. It has been verified, that spacecraft system survivability predictions using standard NASA models of the space radiation environment and conventional methods for dosage and shielding computation, are in very close agreement for proton and high energy electron fluences and are within a factor of 2-3 for electrons of lower energies.
3. It has been shown, that the spherical dose calculation method will best approximate, on the conservative side, the real exposure for all shield thicknesses. For thinner shields this computational method yields results which are above those measured by less than a factor of two.

## Acknowledgments

The CREM electronics box was designed and built by the Space Physics Research Laboratory of the University of Michigan. Dennis L. Haseltine was project engineer, Walter H. Pincus designed the analog circuitry, and John Maurer designed the power supply. The CREM sensor assembly was designed and built at the Goddard Space Flight Center. David K. Studnick did the mechanical design and Dennis R. Hewitt did the thermal design.

Data acquisition software for the CREM experiment was done at Goddard Space Flight Center by William L. Mocarsky and Norman R. Beard, Jr.

The authors wish to thank AE Project Manager, David W. Grimes, AE Experiment Manager James A. Findlay and AE Project Scientist Nelson W. Spencer for their interest in and support of the CREM experiment.

The assistance of Mr. Sidney S. Brashears and Mr. Dee Ho Chang in conducting the CREM on-the-ground simulation experiment and plotting the data, is also greatly acknowledged.

## References

1. Danchenko, V., and U. D. Desai, "Effects of Electric Fields and Their Configurations on Thermal Annealing of MOSFETs and Radiation Hardening", Symp. on Rad. Effects in Semicond. Components, Toulouse, France, March 1967.
2. Hassit, A., and C. E. McIlwain, "Computer Programs for the Computation of B and L (May 1966)", Data User's Note NSSDC 67-27, National Space Science Data Center, Greenbelt, Maryland, March, 1967.
3. Stassinopoulos, E. G., and G. D. Mead, "ALLMAG, GDALMG, LINTRA: Computer Programs for Geomagnetic Field and Field-line Calculations", NSSDC 72-12, National Space Science Data Center, Greenbelt, Maryland, February, 1972.
4. Cain, J. C., and S. J. Cain, "Derivation of the International Geomagnetic Reference Field (IGRF 10/68)", NASA Technical Note TN D-6237, August, 1971.
5. Stassinopoulos, E. G., and C. Z. Gregory, "UNIFLUX: A Unified Orbital Flux Integration and Analysis System", to be published in 1976.

6. Singley, G. W., and J. I. Vette, "The AE4 Model of the Outer Radiation Zone Electron Environment", NSSDC 72-06, National Space Science Data Center, Greenbelt, Maryland, August, 1972.
7. Lavine, J. P., and J. I. Vette, Models of the Trapped Radiation Environment, Volume V: Inner Belt Protons, NASA SP-3024, 1969.
8. Lavine, J. P., and J. I. Vette, Models of the Trapped Radiation Environment, Volume VI: High Energy Protons, NASA SP-3024, 1970.
9. Teague, M. J., and E. G. Stassinopoulos, "A Model of the Starfish Flux in the Inner Radiation Zone", NASA-GSFC Report X-601-72-487, December, 1972.
10. Brucker, G. J., R. S. Ohanian, and E. G. Stassinopoulos, "Successful Large-Scale Use of CMOS Devices on Spacecraft Traveling Through Intense Radiation Belts", IEEE Trans. On Aerospace and Electronic System, Vol. AES-12, No. 1, January, 1976.
11. Liley, B., and S. C. Hamilton, Modified Volume Dose Program (MEVDP), North American Rockwell Eng. Technical Report AFWL-TR-69-68, March, 1971.
12. Private Communication with Captain D. Hollars, Air Force Weapons Laboratory (AFWL), June, 1976.
13. Private Communication with Lt. J. Morel, Air Force Weapons Laboratory (AFWL), June, 1976.
14. Halbleib, Sr., J. A. and W. H. Vandevender, "TIGER: A One-Dimensional Multilayer, Electron/Photon Monte Carlo Transport Code", SLA-73-1026; Sandia Laboratories, March, 1974.
15. Danchenko, V., U. D. Desai, and S. S. Brashears, "Characteristic of Thermal Annealing of Radiation Damage in MOSFETs", J. Appl. Phys., 39, 2416 (1968).
16. Brucker, G. J., "Transient and Steady-State Radiation Response of CMOS/SOS", IEEE Trans. Nucl. Science, NS-21, 6, December, 1974.
17. Teague, M. J., and J. I. Vette, "The Inner Zone Electron Model AE5", NSSDC 72-10, National Space Science Data Center, Greenbelt, Maryland, September, 1972.